Influence of the architecture of magma-poor hyperextended rifted margins on orogens produced by the closure of narrow versus wide oceans

Pauline Chenin, Gianreto Manatschal, Suzanne Picazo, Othmar Müntener, Garry D. Karner, Christopher Johnson, Marc Ulrich

Influence of the architecture of magma-poor hyperextended rifted margins on orogens produced by the closure of 'narrow' versus 'wide' oceans

Pauline Chenin*,[1], Gianreto Manatschal[1], Suzanne Picazo[2], Othmar Müntener[2], Garry Karner[3], Christopher Johnson[3] & Marc Ulrich[1]

[1] CNRS - IPGS - EOST, Université de Strasbourg, 1 rue Blessig, 67084 Strasbourg, France

[2] University of Lausanne, Institut des Sciences de la Terre, Bâtiment Géopolis CH-1015 Lausanne, Switzerland

[3] ExxonMobil, URC/Basin and Petroleum Systems Analysis, Hydrocarbon Systems, Houston campus, Science 1

* Corresponding author (email: chenin@unistra.fr)

Abstract

Orogens resulting from the closure of 'narrow oceans' such as the Alps or the Pyrenees usually lack voluminous syn-subduction and syn-orogenic magmatism. Such orogenies are essentially controlled by mechanical processes in which the initial architecture of the original rifted margins strongly controls the architecture of the orogen. In this paper, we first provide a synthesis of the structure, dimensions and lithology of hyperextended rift systems and oceans, based on recent seismic and petrologic data. Secondly, we investigate how rift-related inheritance influences the crustal geometry and mantle geochemistry of orogens related to the closure of 'narrow oceans', and compare them to orogens resulting from the closure of 'wide/mature oceans'.

Our results show that 'narrow oceans' usually lack mature spreading system forming Penrose-type oceanic crust (i.e. 6–7-km-thick basaltic oceanic crust typical of steady-state spreading systems; see Anonymous, 1972), in contrast to 'wide oceans'. However, there is statistically no difference in the structural and lithological architecture of their passive continental margins. Thus, the main difference between 'narrow' and 'wide oceans' is whether the margins are separated by a significant amount of oceanic crust and underlying depleted mantle. In addition, due to the lack of significant magmatism during the closure of 'narrow oceans', the mantle wedge is likely to remain relatively fertile compared to the wedge above long-lasting subductions of 'wide oceans'. This difference in mantle

composition may dictate the magmatic budget of subsequent orogenic collapse or rifting events.

1 Introduction

Collisional orogens are often regarded as the result from the telescoping of former rifted margins following subduction of a wide oceanic domain (e.g. Uyeda, 1981; Willett et al., 1993; Ernst, 2005; Handy et al., 2010). Long-lasting, Pacific-type subduction systems are typically associated with volcanic arcs and high temperature/low pressure metamorphism in the hanging wall, both of which strongly modify the architecture, lithology and thermal state of the initial margin (Miyashiro, 1961, 1967; Ernst et al., 1970; Gerya, 2011). Therefore, following the closure of a 'wide ocean', at least one side of the orogen is significantly overprinted by subduction-induced processes. This may explain why, except for a few studies (De Graciansky et al., 2011; Butler et al., 2006; Butler, 2013; Mohn et al., 2011, 2014; Beltrando et al., 2014; Tugend et al., 2015, and references therein), little attention has been paid to the potential impact of the initial architecture of the intervening rifted margins. However, orogens such as the Alps, the Pyrenees and the Variscides of Western Europe supposedly result from the closure of 'narrow', possibly 'embryonic' oceans (i.e. devoid of a mature seafloor spreading system; Vlaar and Cloetingh (1984); Pognante et al. (1986); Rosenbaum and Lister (2005); Mohn et al. (2010)) and lack evidence for voluminous arc magmatism contemporaneous with subduction. These orogenies were essentially controlled by mechanical processes, where the architecture of the initial margins dictated largely the architecture of the resulting orogen (see Roca et al. (2011); Beltrando et al. (2014) for reviews). Therefore, the knowledge of the structure, dimensions and lithology of rifted margins and oceans is of primary importance for the understanding and the modelling of collisional orogens.

This paper aims to provide a synthesis of the first-order characteristics of hyperextended rift systems and oceans, at a scale and resolution compatible with lithospheric-scale thermo-mechanical numerical codes. First of all, based on recent seismic and petrologic data, we synthesize the structure and lithology of magma-poor hyperextended rifted margins and oceans, and provide a compilation of the dimensions of the different structural domains comprising rifted margins. We compare the characteristics between 'narrow'/'immature' and 'wide'/'mature oceans'. We define 'narrow oceans' as rift systems that reached at least the stage of hyperextension (see Sutra et al. (2013) and Doré and Lundin (2015) for the definition and a review of *hyperextension*), but remained less than $\sim$ 300 km wide

(the reasons for this limit are discussed below). We use the term 'mature' for oceans that comprise a self-sustaining, steady-state seafloor spreading system, as opposed to 'immature' or 'embryonic' oceans whose development stopped at the stage of hyperextension or exhumation. Second, we investigate how the first-order rift-related inheritance of narrow oceans may influence orogens resulting from their closure, and compare these 'immature orogens' with classical 'mature orogens' produced by the closure of wide/mature oceans (Uyeda, 1981).

2 Characteristics of magma-poor hyperextended rifted margins

Observations of rift systems indicate that during the early stages of rifting extension is often distributed across a relatively wide zone containing multiple rifts (Withjack et al., 1998; Skogseid, 2010). These observations can be compared with the numerical models by Braun and Beaumont (1989); Beaumont and Ings (2012); Chenin and Beaumont (2013); Harry and Grandell (2007), which show that, while the crust is decoupled from the mantle, extension may be accommodated by several inherited crustal weak zones at the same time. Consequently, a series of 'failed rift' basins, which may be offset from the locus of the final breakup, develop in the early stages of extension. Once the crust is coupled to the mantle, extension localizes in one basin while the others are abandoned. During this stage, the crust and lithospheric mantle are progressively thinned, until the eventual lithospheric breakup occurs.

Recent studies suggest that most rifted margins whose necking and hyperextension phases were magma-poor display a similar succession of comparable domains (Figure 1), regardless of whether or not they achieved lithospheric breakup and steady-state seafloor spreading (Sutra et al., 2013; Péron-Pinvidic et al., 2013). In this section, we characterize the first-order architecture and lithology of such rift systems and quantify the width of their distal sub-domains based on natural examples.

2.1 Primary architecture

Since the extensive seismic and drilling surveys of the 90's, rifted margins are no longer regarded as a simple series of tilted blocks adjacent to Penrose-type oceanic crust (6–7-km-thick basaltic oceanic crust typical of steady-state spreading systems; see Anonymous, 1972). Indeed, the drilling of exhumed mantle offshore Iberia led to the reconsideration

of the architecture of rifted margins (Boillot et al., 1980). In order to characterize the architecture of hyperextended rifted margins, Sutra et al. (2013) distinguished several domains based on morphological criteria (Figure 1). On the one hand, the *proximal domain* corresponds to un-thinned or minor extended ($\sim$ 30–35 km thick) continental crust and is characterized by parallel, roughly flat basement and Moho topographies. On the other hand, a typical *oceanic domain* is made of homogeneous, Penrose-type oceanic crust, about 6–7 km thick. Here again, basement and Moho are parallel. The *distal domain*, between them, records most of the rift-related deformation.

The distal domain can be divided into several sub-domains (Figure 1), namely: (a) a *necking domain* characterized by the abrupt thinning of the continental crust from $\sim$ 30–35 km down to $\sim$ 10 km, which translates to a deepening of top basement and shallowing of the Moho (the latter only on seismic sections in depth); (b) a *hyperextended domain*, where continental crust is thinned from $\sim$ 10 km down to 0 km. The transition between the necking and hyperextended domain corresponds to a sudden decrease in the dip of the Moho on depth seismic sections; (c) a so-called *exhumation domain* may exist in magma-poor rifted margins when lithospheric sub-continental mantle is exhumed at the seafloor (Boillot et al., 1987; Whitmarsh et al., 2001; Manatschal and Müntener, 2009). Mantle exhumation is associated with serpentinization down to a depth of 4–6 km (Boillot et al., 1989; Escartín et al., 2001; Minshull et al., 1998), and the transition from serpentinized mantle to fresh peridotite translates to a progressive increase in seismic velocity (Horen et al., 1996; Miller and Christensen, 1997; Skelton et al., 2005). Mantle exhumation may also be accompanied with the emplacement of discontinuous extrusive magmatic rocks from an immature spreading system, which is characterized by incomplete development of oceanic layers 2 and 3 (e.g. Desmurs et al., 2002; Müntener et al., 2004; Jagoutz et al., 2007). Note that allochthonous blocks of continental crust may be found on top of the serpentinized exhumed mantle of the exhumation domain. Thus, on seismic sections, the exhumation domain appears as a more or less structured surface either devoid of a Moho reflector, or with a discontinuous seismic Moho reflector when accompanied with magmatism (Whitmarsh et al., 2001). The transition from the exhumation domain into the oceanic domain is highlighted by an abrupt step-up in the basement (Bronner et al., 2011), which reflects the decrease in the density of the lithospheric column resulting from the production of thicker oceanic crust through increased magmatic activity. In contrast, in the case of magma-rich margins, the transition from thickened magmatic crust to steady-state seafloor spreading is expressed as a step down onto oceanic crust. The first-order morphology of magma-poor

rifted margins is highlighted by the red lines on Figure 1.

2.2 Dimensions and maturity of rift systems

In order to assess the dimensions of rift systems and their distal sub-domains, in addition to their maturity, we first compile the *width* and the lithology of basement rocks for several narrow and wide extensional systems around the world (Table 1). In this paper, the width of an extensional system refers to the distance between the two conjugate necking points (Figure 1). From our compilation (Table 1), we suggest that extensional systems narrower than 300 km are usually immature, that is devoid of a self-sustained, steady-state spreading system, and are floored with either thinned continental crust, exhumed mantle and/or embryonic oceanic crust (Table 1). Note, however, that for rift systems whose development is accompanied by a plume, such as the eastern Gulf of Aden and the southern Red Sea, the rifted margins may be narrower and seafloor spreading may start earlier.

Second, we measure the width of the distal sub-domains (namely the necking, hyperextended and exhumation domains) for a selection of published seismic sections (Table 2). For this compilation, we only consider dip seismic lines imaging extensional systems formed in a single, unidirectional and continuous rifting event (i.e. no significant time lag without extension). Note that the necking domain of the ISE1 seismic section seems anomalously wide compared to the other data points (see Figure 2 b). Its unique architecture displaying a 'double neck' (see seismic section 2 in Table 2) suggests that it did not form in a single extensional event, since deformation tends to become more and more localized as extension progresses. Therefore, we remove this data point in the statistical diagrams c, d, e, f and g of Figure 2, but we include it in our discussion with the asterisk.

In addition, we restrict our measurements to domains with minor magmatic additions. Note that we did not include the width of the exhumation domain for rift basins that did not achieve lithospheric breakup, because in this case the full width of the exhumation domain is not realized.

Figure 2 (c) shows that the width of the distal domain ranges from about 130 to 240 km (or to *350 km), with an average of 170 km (*185 km) and a median of 165 km (*165 km). Of all the distal sub-domains, the necking and exhumation domains have the highest variability in width (see Figure 2 d and f). The width of the necking domain ranges from about 10 to 100 km (or to *210 km) with an average $\sim$ 55 km (*60 km), a median $\sim$ 50 km and a standard deviation of 25 km (*40 km). The width of the exhumation domain varies

between about 20 km to 110 km, with an average of 60 km, a median of $\sim$ 70 km and a standard deviation of $\sim$ 30 km. In contrast, the width of the hyperextended domain seems more constant, varying between 20 and 70 km and with an average of 50 km (median $\sim$ 60 km; standard deviation 15 km). In addition, Figure 2 (e) indicates that no correlation exists between the width of any of the distal sub-domains and the total width of the distal domain. This means that magma-poor hyperextended rifted margins, and hence each of their comprising distal sub-domains, have a specific range of width and can therefore be described with an 'average structural architecture' (see the middle panel of Figure 3 a).

Figure 2 (g) suggests that the width of both the necking and hyperextended domains is unrelated to the maturity of the extensional system, thus to whether it is a 'narrow' or a 'wide' ocean. Therefore, the distal sub-domains of narrow/immature oceans have a structural architecture similar to those of wide/mature oceans (compare the middle panels of Figure 3 a and b).

2.3 First-order lithological architecture

Although rifting affects an initially more or less horizontally homogeneous lithosphere ('layer-cake' lithosphere), tectonic processes and local fluid-rock interactions (including magma) may increasingly modify the lithology and thermal state, and thus the rheology, of the intervening lithosphere as extension progresses.

When rifting is not triggered by magmatism (for example, upwelling of a mantle plume), the lithology of the crust is not significantly modified by extension in the proximal domain and in the necking domain. Therefore, the continental crust of both domains can be approximated by a quartzo-feldspathic material, as usually considered by numerical modellers. Note that, in the necking domain, the ductile layers are mechanically attenuated during extension, so that the crust is fully brittle in the hyperextended domain (Pérez-Gussinyé et al. (2003); Sutra et al. (2013); Manatschal et al. (2015); see the bottom panel of Figure 3 a and b). In addition, the subcontinental mantle underlying the proximal and necking domains is not significantly modified and can be approximated by an average 'inherited mantle' consisting of peridotite with highly variable composition ($\sim$ 50–70% olivine (ol), $\sim$ 1–30 % clinopyroxene (cpx), $\sim$ 20–30% orthopyroxene (opx) and $\sim$ 1–4% spinel (sp); Müntener et al. (2010); Picazo et al. (2016)) and pyroxenite (ol as low as 0%, cpx up to 80%, opx up to 60% and 1–2% spinel/garnet).

In contrast, in hyperextended and exhumation domains, fluid-rock interactions form hy-

drous minerals, similar to the fluid-rock interactions observed in present-day mid-oceanic ridges (Mével, 2003; Bach et al., 2004; Boschi et al., 2006; Picazo et al., 2012, 2013). Hydrothermal circulation is responsible for the formation of hydrous minerals within hyperextended crust (e.g. sericite and illite; Pinto (2014) and references therein), as well as in exhumed mantle (e.g. serpentinite, chlorite, talc; see Hess (1955); Christensen (1970); Früh-Green et al. (2004); Picazo et al. (2013)). Therefore, the rheology of the hyperextended continental crust and the top 4–6 km of lithospheric mantle in the exhumation domain can be approximated by a phyllosilicate-type rheology.

Significant crustal thinning is also associated with partial melting of the asthenosphere (Latin and White, 1990). The resulting melts are initially not, or only little extracted, but impregnate the overlying lithospheric mantle in the hyperextended domain (Müntener et al., 2010). Thus, the subcontinental mantle underlying the hyperextended crust and exhumed mantle displays a 'fertile' composition with a significant amount of plagioclase and clinoypyroxene, and evidence for melt rock reaction (e.g. Müntener and Piccardo, 2003; Müntener et al., 2010). As a consequence, immature rift systems whose development stopped at the stage of hyperextension are likely to retain this fertile mantle composition (Figure 3 b, bottom panel).

In contrast, during lithospheric breakup, melt starts to be extracted and a sustainable magmatic system is established marking the onset of steady-state seafloor spreading. The resulting oceanic crust is homogeneous in both composition and thickness (basaltic to gabbroic and $\sim$ 6–7 km thick; Anonymous (1972)). The process of partial melting associated with the creation of oceanic crust depletes the underlying mantle in the most fusible elements, leaving an average composition of 57% ol, 13% cpx, 28% opx and 2% sp (i.e. a 'depleted DMM' (DMM = Depleted MORB Mantle); see Workman and Hart (2005) and Figure 3 a, bottom panel). Note that, even in the case of a so-called *magma-poor rifting*, onset of steady-state seafloor spreading is presumably triggered by a magmatic pulse (Bronner et al., 2011). Therefore, we expect the mantle underlying the most distal part of the margins of mature oceans to be depleted in fusible elements, conversely to the mantle underlying immature oceans.

We calculated the density of fertile and depleted mantle 700°C to 1300°C in steps of 100°C, at pressure from 0.5 to 3 GPa (Table 3) based on their average modal composition (Müntener et al., 2010; McCarthy and Müntener, 2015), their physical properties (Hacker et al., 2003) and the geotherm of each mantle-type domain (Sclater et al., 1980). At pressure of 0.5 GPa, calculations show that fertile plagioclase peridotite is less dense than

depleted harzburgite. From 1.0 to 2 GPa, depleted mantle is lighter by about 20–30 kg.m^{-3} compared to fertile mantle. Note that the peridotites considered in this calculation are relatively rich in Fe, but if they would be richer in Mg, the density contrast would be of the order of 50–80 kg.m^{-3}. At high pressures, because of the higher modal abundance of garnet in fertile rocks, the fertile peridotite is denser than the residual harzburgite by about 30–40 kg.m^{-3}.

The density contrasts observed between fresh versus altered peridotites and depleted vs. fertile mantle are significant enough to influence tectonic processes as shown for example for basin subsidence (Kaus et al., 2005). In particular the location of subduction initiation during the inversion of an ocean may be controlled by such density contrasts.

3 First-order architecture of collisional orogens

Every ocean will eventually undergo subduction and be sutured after collision of its continental margins. On a first-order, a collisional orogen can be regarded as a three-part system comprising (Figure 4 a2 and b2): (1) two buttresses; (2) an accretionary wedge; and (3) a subducted part.

In this section, we discuss how these different components may correlate with specific parts of the initial rift system. In order to avoid the complexity induced by magmatic overprinting, we focus on the well-studied Pyrenean and Alpine orogens, both of which largely lack voluminous syn-subduction and syn-orogenic magmatism and are therefore essentially controlled by mechanical processes. Moreover, as both are relatively recent, their orogenic architecture is fairly well-preserved.

Oceanic lithosphere, due to its high density, tends to be efficiently subducted. According to Stern (2004), most of the ophiolites preserved within orogens correspond to obducted remnants of buoyant oceanic crust from small and young oceanic basins, usually former forearcs or backarcs, rather than mature oceanic crust. Besides, a significant proportion of sediments is also usually subducted, while the remaining part accumulates in the accretionary prism (Clift et al., 2004; Stern, 2011, and references therein). A significant proportion of the subducted material has to be integrated to the orogenic root in order to account for the isostasy of collisional orogens, however the deep architecture of collisional orogens is very poorly constrained (Butler, 2013) as illustrated by the diversity in the interpretation of the deep part of the ECORS-CROP seismic section (Figure 5 b).

Besides, both the Alpine and the Pyrenean orogens display a similar architecture, where the external domain is made of little deformed continental basement and the internal part

of a complex stacking of material originating from the distal margin (De Graciansky et al., 2011; Bellahsen et al., 2014; Butler et al., 2006; Butler, 2013; Schmid et al., 2004; Beltrando et al., 2014; Casteras, 1933; Mattauer, 1968; Jammes et al., 2009; Muñoz, 1992). Recent studies (Mohn et al., 2014; Tugend et al., 2015) show consistently that the external parts of the orogen (the buttresses B on Figure 4) correspond to the little deformed necking zones of the former continental margins. In contrast, the internal part corresponds to the accretionary prism (A on Figure 4), which is comprised of thinned continental basement remnants, ophiolites and/or exhumed mantle and thick sequences of highly deformed sediments (see Beltrando et al. (2014) for a review). This accreted material is essentially derived from the sedimentary cover, but according to Andersen et al. (2012), some parts of the hyperextended and exhumation domains may also be integrated into the accretionary wedge, as evidenced by the remnants of exhumed mantle in the Caledonian orogen (see also Chew and Van Staal (2014). This proposition is also verified in the Alps and in the Pyrenees, where most ophiolites are remnants from 'inherited' or 'refertilized' subcontinental mantle rather than from a steady-state spreading system (Lemoine et al., 1987; Müntener et al., 2010; Picazo et al., 2016).

What controls the distribution of accreted versus subducted material remains poorly constrained. From the seismic refraction profile across offshore Iberia and the interpretation of an adjacent transect calibrated by drill holes shown in Figure 5 (a), we speculate that the boundary between sediments and hydrated material on the one hand (green and blue colors on the refraction profile) and the unaltered underlying mantle on the other may act as a decollement separating the accreted and subducted part once the hyperextended and exhumation domains reach the subduction trench.

The heat budget is significantly different between mature and immature subductions/orogens. Indeed, in mature subduction systems, a large amount of heat is advected by the magma transported from the mantle to the crust, inducing arc magmatism and batholith formation in the hanging wall of the subduction (Uyeda, 1981; Stern, 2002). The associated fluids and magma transported into the overlying crust weaken it considerably (Gerya, 2011), which has a major impact on the architecture of the subsequent orogen (Figure 4 a).

In contrast, although high-grade metamorphism is recorded in the Alps (for instance in the Tauern window and the Lepontine dome), heat transfer from the mantle is limited. The metamorphic belts of Alpine-type systems are created by stacking upper continental crustal slivers and internal heat production by radioactive decay (Burg and Gerya, 2005). The resulting metamorphism may have some impact on the rheology of the buried crust

(Bellahsen et al., 2014), but is not significant enough to affect the overall architecture of the orogen (Figure 4 b). Therefore, in our study, we neglect the effects of low-grade metamorphism in immature orogens.

In summary, when the closure of a (narrow) ocean is devoid of significant magmatism, the orogenesis is essentially controlled by mechanical processes and its first-order geometry can be related to specific portions of the initial rift system (Figure 4): (1) the buttresses correspond to the proximal plus necking domains (see Figure 1); (2) the accretionary prism to part of the hyperextended and/or exhumation domains, in addition to part of the overall basin sediments; and (3) the subducted part to most of the hyperextended and exhumation domains, the oceanic lithosphere and part of the distal and oceanic sediments.

4 Discussion

Since the advent of plate tectonics and the understanding of first-order subduction processes, collisional orogens are usually regarded as the result of the telescoping of continental margins after long-lasting subduction of a wide oceanic domain (Uyeda, 1981; Willett et al., 1993; Ernst, 2005; Handy et al., 2010). Such orogens are characterized by paired metamorphic belts, namely a low temperature/high pressure belt corresponding to the accretionary wedge; and a high temperature/low pressure belt related to arc metamorphism and/or magmatism (Miyashiro, 1961; Dewey and Horsfield, 1970; Brown, 2009, and references therein). However, several collisional orogens such as the Alps and the Pyrenees lack voluminous magmatism contemporaneous to subduction, that is, are devoid of remnants of arcs, forearcs and backarcs and of high temperature/low pressure metamorphic assemblages in the upper plate. Yet, both orogens result from the closure of relatively narrow ($<$ 400–600 km for the Alpine Tethys, $<$ 200 km for the Pyrenean rift system), hyperextended (Pyrenean rift system) or possibly embryonic (Alpine Tethys) 'oceans' (Rosenbaum et al., 2002; Rosenbaum and Lister, 2005; Mohn et al., 2010; Lemoine et al., 1987). This may be the main cause for the lack of significant magmatic products. Indeed, because significant dehydration of the basaltic crust and serpentinized mantle starts only from a depth of 100–200 km (Peacock et al., 1994; Rüpke et al., 2004), a magmatic arc is unlikely to develop before the slab is subducted to this depth (e.g. Jarrard, 1986; England et al., 2004). Therefore, there must be a critical width for rift systems, below which their subduction is devoid of significant magmatic activity. In such cases, the subsequent orogenies may be essentially controlled by mechanical processes, in which the structural and lithologic architecture of the intervening margins may be the dominant factor in controlling the architecture of the

orogen.

4.1 'Narrow oceans' and 'magma-poor' subduction

As slabs subduct with an average dip of 50–60° in the upper mantle (Stevenson and Turner, 1977; Tovish et al., 1978; Billen, 2008), the slab must be at least 130 km long to reach a depth of 100 km. Adding to this twice the 55 km average length of each necking domain (section 2.1), which is usually not subducted (section 3), magma generation seems very unlikely during closure of rift systems narrower than 240 km. Furthermore, subduction must last long enough for a sufficient amount of volatiles to induce hydrous partial melting (Peacock, 1991; Gaetani and Grove, 1998). This is consistent with the compilation by Jarrard (1986), which shows that the length of the subducted slab associated with the youngest arc (the Philippines arc, 6 m.y. old) is at least 170 km long. As a consequence, we expect rift basins narrower than 300 km to be devoid of significant magmatism expressed at the surface. In the following, we refer to these as *narrow oceans*, as opposed to *wide oceans* larger than $\sim$ 1,000 km.

In addition to this 'flux melting', arc magma generation is also driven by decompression melting of the hot asthenosphere rising to compensate the down-dragging of mantle wedge material by the slab (Iwamori, 1998; Jagoutz et al., 2011; Sisson and Bronto, 1998). Yet, decompression melting becomes important only when vigorous convection is active in the mantle wedge, which only develops after significant subduction (Peacock et al., 1994; Conder et al., 2002). Thus, it is unlikely to occur during the closure of a narrow ocean.

4.2 Characteristics of 'narrow' versus 'wide' oceans

As highlighted in Table 1, extensional systems narrower than 300 km are usually devoid of a mature, self-sustaining spreading system, thus of 'normal' oceanic crust. As a result, their seafloor is either comprised of thinned continental crust, exhumed mantle and/or embryonic oceanic crust. On the contrary, mature, steady-state oceanic systems are usually characterized by a homogeneous, Penrose-type oceanic crust. Of course, there is a wide range of oceanic crust types between these 'embryonic' and 'Penrose' end-members. For instance, in ultra-slow spreading systems, a thin (2–5 km thick) 'oceanic crust' comprised of both magmatic and a-magmatic segments may be steadily emplaced for millions of years (Dick et al., 2003). Yet, like normal oceanic crust, oceanic crust formed at ultra-slow spreading ridges is most likely to be efficiently subducted during the closure of wide oceans (Stern, 2004), thus it will *a priori* not influence the subsequent orogeny.

As we showed in section 2.1, there is statistically no relationship between the size or maturity of a magma-poor hyperextended rift system and the architecture of its margins. Therefore, on a first-order, the main difference between narrow and wide oceans is the existence of a significant amount of oceanic crust and underlying depleted mantle (compare Figure 3 a and b). In contrast, the mantle underlying narrow embryonic oceans is likely to retain its fertile composition resulting from the impregnation by asthenospheric melts during hyperextension (Müntener et al., 2010).

4.3 Subduction of 'narrow' versus 'wide oceans' and subsequent orogenies

During short-lived subduction associated with the closure of narrow 'oceans', the slab remains at relatively shallow angle (Billen, 2008) and no self-sustaining subduction will likely develop due to insufficient slab pull (Hall et al., 2003; Gurnis et al., 2004), thus development of small-scale convection above the subducting slab is unlikely (Peacock et al., 1994). Furthermore, the small length of the slab may not allow for a significant amount of volatiles to reach the critical depth for entering the hot part of the mantle wedge (Rüpke et al., 2004; Grove et al., 2006). In such circumstances, the generation of arc magmas is limited and hydration of the mantle wedge is likely to be the dominant process (Peacock et al., 1994).

In addition, because of the low dip angle of the slab, both slab pull and the potential effect of mantle flow on the slab are limited, making the development of backarc basins unlikely (Uyeda, 1981; Heuret and Lallemand, 2005). This is supported by the worldwide compilation of backarc deformation style by Heuret and Lallemand (2005), which highlights that no young subduction is associated with strongly extensional backarc settings. Therefore, the lithosphere underlying orogens resulting from the closure of narrow oceans is likely to be relatively fertile and hydrated (Figure 6 b).

In contrast, protracted subduction associated with the closure of wide oceans is likely to become self-sustained, in particular, due to the eclogitization of the subducting slab, which makes it denser than the encompassing asthenospheric mantle (Doin and Henry, 2001; Aoki and Takahashi, 2004). Long lasting subduction develops usually vigorous convection in the mantle wedge, which efficiently transports volatiles derived from the dehydration of the slab to great depth (Peacock et al., 1994). The resulting partial melting creates thickened sialic crust at the surface (magmatic arcs), induces high-temperature metamorphism in the encompassing upper plate and depletes the underlying mantle in fusible elements (Uyeda,

1981).

When a significant amount of oceanic lithosphere is subducted, the strong slab pull, and potentially the effect of dynamic mantle flow dragging on the slab may induce a backward migration of the lower plate with respect to the upper plate (slab rollback), which may help form backarc basins (Uyeda, 1981; Heuret and Lallemand, 2005). In such cases, back-arc extension may be associated with seafloor spreading and underlying mantle depletion as well. Note that, while vigorous convection within the mantle wedge tends to homogenize its composition, a lower mantle fertility is still to be expected beneath an orogen resulting from the closure of a wide ocean. This assumption is supported by the depleted mantle wedge composition of the Pacific subduction compiled by Woodhead et al. (1993) and the decrease in mantle fertility with increasing distance to the arc region observed in the Lau and Mariana backarc regions (Martinez and Taylor, 2002). Therefore, the thermal and lithological architecture of orogens related to the closure of wide oceans may largely differ from thermal and lithological architecture of their initial margins, as opposed to orogens consequent upon the closure of narrow oceans (compare Figure 6 a and b).

4.4 Impact on subsequent collapse or rifting magmatic budget

The difference in mantle composition resulting from the closure of narrow/embryonic oceans versus wide oceans may dictate the magmatic budget of subsequent extensional events such as post-orogenic collapse or rifting. Indeed, the depleted mantle beneath orogens related to mature subduction systems may not allow for voluminous magma production, in contrast to the fertile mantle underlying orogens produced by the closure of narrow oceans. This hypothesis may account for both the a-magmatic collapse of the Scandinavian Caledonides and the large amount of magmatism during the Variscan orogenic collapse.

The Variscides of Western Europe result from the closure of several narrow 'oceans' (McKerrow et al., 2000a; Franke, 2006), in addition to the suturing of the wide ($>$ 2,000 km; Torsvik, 1998; Nance and Linnemann, 2008) Rheic Ocean (see Matte (2001) and Kröner and Romer (2013) for reviews). Only the closure of the Rheic Ocean did presumably form a significant magmatic arc (Franke, 2006). The orogenic collapse of the Variscan topography was followed by significant magmatic activity, which resulted in widespread, more or less acidic intrusions within the crust, and formed a thick mafic crustal underplating across most of the orogenic area (Bois et al., 1989; Rey, 1993; Costa and Rey, 1995; Schaltegger, 1997; Petri, 2014).

In contrast, the Scandinavian Caledonides between Norway and Greenland resulted essentially from the closure of the wide (> 2,000 km; van Staal et al., 2012) Iapetus Ocean (McKerrow et al., 2000b). At this latitude, the two-sided subduction of this ocean formed at least one major volcanic arc now exposed in Norway (Mac Niocaill et al., 1997; McKerrow et al., 2000b). Note that, further South, the British and Appalachian Caledonides involved many more micro-continents, narrow oceanic tracks and volcanic arcs (see Roberts (2003); Chew and Van Staal (2014) and Figure 1 in van Staal et al. (2012)), comparably to the Variscides of Western Europe (see Figure 2 in Franke (2006)). Thus we restrict our consideration of the Scandinavian Caledonides to the norther part between Norway and Greenland, where accretion of terranes was extremely limited. The Caledonian topography underwent a phase of orogenic collapse, which was essentially achieved through mechanical deformation without significant magmatic activity north of the Elbe lineament (McClay et al., 1986; Andersen, 1998; Meissner, 1999; Fossen et al., 2014).

An alternative hypothesis to account for the low magmatic budget of the Caledonian orogenic collapse relies on the depleted composition of the mantle underlying the two continents involved in the orogeny, namely Laurentia and Baltica. Indeed, both are comprised of Archean cratonic cores (the North American and East European craton, respectively), which are characterized by a thick, cold and depleted lithospheric mantle (Bernstein et al., 1998; Griffin et al., 2003; Beyer et al., 2004).

The importance of the magmatic event associated with a post-orogenic collapse has direct consequences on the characteristics of the lithosphere, since it may erase all the structural inheritance in the lower crust (Bois et al., 1989; Rey, 1993), introduce major compositional and thermal heterogeneities in the upper and middle crust (Costa and Rey, 1995; Vanderhaeghe and Teyssier, 2001), and significantly deplete the underlying mantle (McCarthy and Müntener, 2015). This inheritance is also much more likely to be expressed in subsequent tectonic events, for instance influencing the localization and controlling the magmatic budget of later rifting events. In particular, this could account for the differing behaviour of the North Atlantic rift with respect to the Caledonian and Variscan orogenic lithospheres highlighted by Chenin et al. (2015). It could also explain the variability in the behaviour of the Gondwanan rifts with respect to the former orogens affecting the supercontinent (i.e. paralleling, cutting across or circumventing; see Krabbendam and Barr (2000)). The characteristics of the narrow hyperextended rift systems and wide oceans morphology, lithology, subduction and resulting orogens are summarized in Table 4 and Figure 6.

5 Conclusion

In this paper, we show that each distal rift domain, as defined by Sutra et al. (2013), has a specific range of width. In contrast to the necking and exhumation domains, whose range of width is large, the width of the hyperextended domain is relatively consistent amongst rifted margins (about 50 km). Both the width of the necking domain and of the hyperextended domain are independent of the total width of the margin (i.e. the distance from the coupling point to the lithospheric breakup point) and of the maturity of the rift system (i.e. whether or not steady-state, self-sustaining seafloor spreading is achieved).

As 'narrow oceans' are usually devoid of mature spreading systems (then called 'immature') in contrast to wide, mature oceans, the main difference between these end-members is whether their margins are separated by a wide domain of 'normal' oceanic crust. Furthermore, narrow and immature 'oceans' are likely to be underlain by fertile mantle resulting from melt impregnation during the phase of hyperextension conversely to wide and mature oceans, which have a typical mid-oceanic ridge-type depleted mantle.

During the subduction of narrow oceans, the slab is expected to remain at shallow angle (Stevenson and Turner, 1977; Tovish et al., 1978; Billen, 2008). Thus, subduction is very unlikely to become self sustained (Hall et al., 2003; Gurnis et al., 2004) or to develop vigorous small-scale convection in the mantle wedge (Peacock et al., 1994), as opposed to subduction of wide oceans. Furthermore, subduction of narrow oceans does not produce significant magmatic activity, thus no mantle depletion, because insufficient volatiles reach a sufficient depth to allow partial melting (Peacock, 1991; Rüpke et al., 2004). Therefore, hydration is likely to be the dominant process in the mantle wedge.

Conversely, protracted subduction associated with the closure of wide oceans develop vigorous convection in the mantle wedge, forms magmatic arcs, and is potentially associated with seafloor spreading in the backarc region (Uyeda, 1981; Peacock et al., 1994). These processes deplete the underlying mantle in fusible elements, create new crustal material and are associated with high temperature/low pressure metamorphism.

As a result, orogens resulting from the closure of narrow oceans may be essentially controlled by mechanical processes, without significant compositional or thermal perturbation, and with a major influence of the inherited characteristics of the intervening margins. In contrast, orogens produced by the closure of wide oceans may be significantly controlled by subduction-induced processes.

Because of the lack of magmatic activity during the closure of narrow oceans, the mantle underlying the resulting orogens is likely more fertile than the mantle underlying orogens

due to the closure of wide oceans. This difference in fertility may dictate the magmatic budget of a subsequent extensional event, such as a post-orogenic collapse or an episode of rifting.

Acknowledgement

We acknowledge careful reviews and helpful comments by C. van Staal, A. G. Leslie and an anonymous reviewer. Constructive comments by N. Bellahsen on a earlier version of the manuscript were also much appreciated. This research was supported by ExxonMobil in the framework of the project CEIBA.

References

Afilhado, A., Matias, L., Shiobara, H., Hirn, A., Mendes-Victor, L., and Shimamura, H. (2008). From unthinned continent to ocean: The deep structure of the West Iberia passive continental margin at 38°N. *Tectonophysics*, 458:9–50.

Andersen, T. B. (1998). Extensional tectonics in the Caledonides of southern Norway, an overview. *Tectonophysics*, 285:333–351.

Andersen, T. B., Corfu, F., Labrousse, L., and Osmundsen, P.-T. (2012). Evidence for hyperextension along the pre-Caledonian margin of Baltica. *Journal of the Geological Society*, 169(5):601–612.

Anonymous (1972). Penrose field conference on ophiolites. In *Penrose Field Conference on ophiolites*, volume 17, pages 24–25. Geotimes.

Aoki, I. and Takahashi, E. (2004). Density of MORB eclogite in the upper mantle. *Physics of the Earth and Planetary Interiors*, 143-144:129–143.

Aslanian, D., Moulin, M., Olivet, J. L., Unternehr, P., Matias, L., Bache, F., Rabineau, M., Nouzé, H., Klingelheofer, F., Contrucci, I., and Labails, C. (2009). Brazilian and African passive margins of the Central Segment of the South Atlantic Ocean: Kinematic constraints. *Tectonophysics*, 468(1-4):98–112.

Bach, W., Garrido, C. J., Paulick, H., Harvey, J., and Rosner, M. (2004). Seawater-peridotite interactions: First insights from ODP Leg 209, MAR 15°N. *Geochemistry, Geophysics, Geosystems*, 5(9):n/a–n/a.

Beaumont, C. and Ings, S. J. (2012). Effect of depleted continental lithosphere counterflow and inherited crustal weakness on rifting of the continental lithosphere: general result. *Journal of Geophysical Research*, 117(B8):n/a–n/a.

Bellahsen, N., Mouthereau, F., Boutoux, A., Bellanger, M., Lacombe, O., Jolivet, L., and Rolland, Y. (2014). Collision kinematics in the western external Alps. *Tectonics*, 33(6):1055–1088.

Beltrando, M., Manatschal, G., Mohn, G., Dal Piaz, G. V., Vitale Brovarone, A., and Masini, E. (2014). Recognizing remnants of magma-poor rifted margins in high-pressure orogenic belts: The Alpine case study. *Earth-Science Reviews*, 131:88–115.

Bernstein, S., Kelemen, P. B., and Brooks, C. (1998). Depleted spinel harzburgite xenoliths in Tertiary dykes from East Greenland: Restites from high degree melting. *Earth and Planetary Science Letters*, 154(1-4):221–235.

Beyer, E. E., Brueckner, H. K., Griffin, W. L., O'Reilly, S. Y., and Graham, S. (2004). Archean mantle fragments in Proterozoic crust, Western Gneiss Region, Norway. *Geology*, 32(7):609–612.

Billen, M. I. (2008). Modeling the dynamics of subducting slabs. *Annual Review of Earth and Planetary Sciences*, 36(1):325–356.

Boillot, G., Féraud, G., Recq, M., and Girardeau, J. (1989). Undercrusting by serpentinite beneath rifted margins. *Nature*, 341(6242):523–525.

Boillot, G., Grimaud, S., Mauffret, A., Mougenot, D., Kornprobst, J., Mergoil-Daniel, J., and Torrent, G. (1980). Ocean-continent boundary off the Iberian margin: A serpentinite diapir west of the Galicia Bank. *Earth and Planetary Science Letters*, 48(1):23–34.

Boillot, G., Recq, M., Winterer, E., Meyer, A., Applegate, J., Baltuck, M., Bergen, J., Comas, M., Davies, T., Dunham, K., Evans, C., Girardeau, J., Goldberg, G., Haggerty, J., Jansa, L., Johnson, J., Kasahara, J., Loreau, J., Luna-Sierra, E., Moullade, M., Ogg, J., Sarti, M., Thurow, J., and Williamson, M. (1987). Tectonic denudation of the upper mantle along passive margins: a model based on drilling results (ODP leg 103, western Galicia margin, Spain). *Tectonophysics*, 132(4):335–342.

Bois, C., Pinet, B., and Roure, F. (1989). Dating lower crustal features in France and adjacent areas from deep seismic profiles. In et al. Mereu, R. F., editor, *Properties and processes of earth's lower crust*, pages 17–31. American Geophysical Union Geophysical Monograph 51.

Boschi, C., Früh-Green, G. L., Delacour, A., Karson, J. A., and Kelley, D. S. (2006). Mass transfer and fluid flow during detachment faulting and development of an oceanic core complex, Atlantis Massif (MAR 30°N). *Geochemistry, Geophysics, Geosystems*, 7(1):n/a–n/a.

Bosworth, W., Huchon, P., and McClay, K. (2005). The Red Sea and Gulf of Aden Basins. *Journal of African Earth Sciences*, 43(1-3):334–378.

Braun, J. and Beaumont, C. (1989). Dynamical models of the role of crustal shear zones in asymmetric continental extension. *Earth and Planetary Science Letters*, 93(3-4):405–423.

563 Bronner, A., Sauter, D., Manatschal, G., Péron-Pinvidic, G., and Munschy, M. (2011).
564 Magmatic breakup as an explanation for magnetic anomalies at magma-poor rifted mar-
565 gins. *Nature Geoscience*, 4:549–553.

566 Brown, M. (2009). Metamorphic patterns in orogenic systems and the geological record.
567 *Geological Society, London, Special Publications*, 318(1):37–74.

568 Burg, J. P. and Gerya, T. V. (2005). The role of viscous heating in Barrovian metamor-
569 phism of collisional orogens: Thermomechanical models and application to the Lepontine
570 Dome in the Central Alps. *Journal of Metamorphic Geology*, 23(2):75–95.

571 Butler, R. W. H. (2013). Area balancing as a test of models for the deep structure of moun-
572 tain belts, with specific reference to the Alps. *Journal of Structural Geology*, 52(1):2–16.

573 Butler, R. W. H., Tavarnelli, E., and Grasso, M. (2006). Structural inheritance in mountain
574 belts: An Alpine-Apennine perspective. *Journal of Structural Geology*, 28(11):1893–
575 1908.

576 Casteras, M. (1933). Recherches sur la structure du versant nord des Pyrénées centrales
577 et orientales. *Bulletin du Service de la Carte Géologique de France*, 37:25.

578 Chenin, P. and Beaumont, C. (2013). Influence of offset weak zones on the development
579 of rift basins: Activation and abandonment during continental extension and breakup.
580 *Journal of Geophysical Research*, 118(4):1698–1720.

581 Chenin, P., Manatschal, G., Lavier, L. L., and Erratt, D. (2015). Assessing the impact
582 of orogenic inheritance on the architecture, timing and magmatic budget of the North
583 Atlantic rift system: a mapping approach. *Journal of the Geological Society*, 172(6):711–
584 720.

585 Chew, D. M. and Van Staal, C. R. (2014). The ocean ‚Äì continent transition zones
586 along the Appalachian ‚Äì Caledonian margin of Laurentia: Examples of large-scale
587 hyperextension during the opening of the Iapetus Ocean. *Geoscience Canada*, 41(2):165.

588 Chian, D., Reid, I. D., and Jackson, H. R. (2001). Crustal structure beneath Orphan Basin
589 and implications for nonvolcanic continental rifting. *Journal of Geophysical Research*,
590 106(B6):10,923–10,940.

591 Christensen, N. I. (1970). Composition and evolution of the oceanic crust. *Marine Geology*,
592 8:139–154.

Clift, P. D., Dewey, J. F., Draut, A. E., Chew, D. M., Mange, M., and Ryan, P. D. (2004). Rapid tectonic exhumation, detachment faulting and orogenic collapse in the Caledonides of western Ireland. *Tectonophysics*, 384(1-4):91–113.

Conder, J. A., Wiens, D. A., and Morris, J. (2002). On the decompression melting structure at volcanic arcs and back-arc spreading centers. *Geophysical Research Letters*, 29(15):17–1–17–4.

Costa, S. and Rey, P. (1995). Lower crustal rejuvenation and growth during post-thickening collapse: Insights from a crustal cross section through a Variscan metamorphic core complex. *Geology*.

De Graciansky, P. C., Roberts, D. G., and Tricart, P. (2011). The Western Alps, from Rift to Passive Margin to Orogenic Belt: An Integrated Geoscience Overview. In *Developments in Earth Surface Processes 14*, page 432p. Elsevier.

Desmurs, L., Müntener, O., and Manatschal, G. (2002). Onset of magmatic accretion within a magma-poor rifted margin: a case study from the Platta ocean-continent transition, eastern Switzerland. *Contributions to Mineralogy and Petrology*, 144(3):365–382.

Dewey, J. F. and Horsfield, B. (1970). Plate tectonics, orogeny and continental growth. *Nature*, 225:521–525.

Dick, H. J. B., Lin, J., and Schouten, H. (2003). An ultraslow-spreading class of ocean ridge. *Nature*, 426(6965):405–412.

Direen, N. G., Stagg, H. M. J., Symonds, P. A., and Colwell, J. B. (2008). Architecture of volcanic rifted margins: new insights from the Exmouth–Gascoyne margin, Western Australia. *Australian Journal of Earth Sciences*, 55(3):341–363.

Doin, M.-P. and Henry, P. (2001). Subduction initiation and continental crust recycling : the roles of rheology and eclogitization. *Tectonophysics*, 342:163–191.

Doré, T. and Lundin, E. (2015). Hyperextended continental margins – Knowns and unknowns. *Geology*, 43(1):95–96.

Edwards, J. (2002). Development of the Hatton–Rockall Basin, North-East Atlantic Ocean. *Marine and Petroleum Geology*, 19(2):193–205.

England, P., Engdahl, R., and Thatcher, W. (2004). Systematic variation in the depths of slabs beneath arc volcanoes. *Geophysical Journal International*, 156(2):377–408.

623 Ernst, W. G. (2005). Alpine and Pacific styles of Phanerozoic mountain building:
624 subduction-zone petrogenesis of continental crust. *Terra Nova*, 17:165–188.

625 Ernst, W. G., Seki, Y., Onuki, H., and Gilbert, M. C. (1970). *Comparative study of low-*
626 *grade metamorphism in the California Coast Ranges and the Outer Metamorphic Belt*
627 *of Japan*, volume 124 of *Geological Society of America Memoirs*. Geological Society of
628 America.

629 Escartín, J., Hirth, G., and Evans, B. (2001). Strength of slightly serpentinized peridotites:
630 Implications for the tectonics of oceanic lithosphere. *Geology*, 29(11):1023–1026.

631 Fossen, H., Gabrielsen, R. H., Faleide, J. I., and Hurich, C. A. (2014). Crustal stretching in
632 the Scandinavian Caledonides as revealed by deep seismic data. *Geology*, 42(9):791–794.

633 Franke, W. (2006). The Variscan orogen in Central Europe: construction and collapse.
634 *Geological Society, London, Memoirs*, 32(1):333–343.

635 Früh-Green, G. L., Connolly, J. A., Plas, A., Kelley, D. S., and Grobéty, B. (2004). Ser-
636 pentinization of oceanic peridotites: Implications for geochemical cycles and biological
637 activity. In Wilcock, W. S., DeLong, E. F., Kelley, D. S., Baross, J. A., and Craig Cary,
638 S., editors, *The subseafloor biosphere at mid-ocean ridges*, volume 144, pages 119–136.
639 American Geophysical Union Geophysical Monograph 144, Washington, D. C.

640 Gaetani, G. A. and Grove, T. L. (1998). The influence of water on melting of mantle
641 peridotite. *Contributions to Mineralogy and Petrology*, 131(4):323–346.

642 Gerya, T. (2011). Future directions in subduction modeling. *Journal of Geodynamics*,
643 52:344–378.

644 Gladczenko, T. P., Skogseid, J., and Eldhom, O. (1998). Namibia volcanic margin. *Marine*
645 *Geophysical Researches*, 20(4):313–341.

646 Griffin, W., O'Reilly, S., Abe, N., Aulbach, S., Davies, R., Pearson, N., Doyle, B., and
647 Kivi, K. (2003). The origin and evolution of Archean lithospheric mantle. *Precambrian*
648 *Research*, 127(1-3):19–41.

649 Grove, T. L., Chatterjee, N., Parman, S. W., and Médard, E. (2006). The influence of
650 H2O on mantle wedge melting. *Earth and Planetary Science Letters*, 249(1-2):74–89.

651 Gurnis, M., Hall, C., and Lavier, L. (2004). Evolving force balance during incipient sub-
652 duction. *Geochemistry, Geophysics, Geosystems*, 5(7).

Hacker, B. R., Abers, G. A., and Peacock, S. M. (2003). Subduction factory 1. Theoretical mineralogy, densities, seismic wave speeds, and H2O contents. *Journal of Geophysical Research*, 108(B1):2029.

Hall, C. E., Gurnis, M., Sdrolias, M., Lavier, L. L., and Müller, R. (2003). Catastrophic initiation of subduction following forced convergence across fracture zones. *Earth and Planetary Science Letters*, 212(1-2):15–30.

Handy, M. R., M. Schmid, S., Bousquet, R., Kissling, E., and Bernoulli, D. (2010). Reconciling plate-tectonic reconstructions of Alpine Tethys with the geological-geophysical record of spreading and subduction in the Alps. *Earth-Science Reviews*, 102(3-4):121–158.

Harry, D. L. and Grandell, S. (2007). A dynamic model of rifting between Galicia Bank and Flemish Cap during the opening of the North Atlantic Ocean. *Geological Society, London, Special Publications*, 282(1):157–172.

Hess, H. (1955). Serpentines, Orogeny, and Epeirogeny. *Geological Society of America Special Papers*, 62:391–408.

Heuret, A. and Lallemand, S. (2005). Plate motions, slab dynamics and back-arc deformation. *Physics of the Earth and Planetary Interiors*, 149(1-2 SPEC. ISS.):31–51.

Horen, H., Zamora, M., and Dubuisson, G. (1996). Seismic waves velocities and anisotropy in serpentinized peridotites from Xigaze ophiolite: abundance of serpentine in slow spreading ridge. *Geophysical Research Letters*, 23(1):9–12.

Iwamori, H. (1998). Transportation of H2O and melting in subduction zones. *Earth and Planetary Science Letters*, 160(1-2):65–80.

Jagoutz, O., Müntener, O., Manatschal, G., Rubatto, D., Péron-Pinvidic, G., Turrin, B. D., and Villa, I. M. (2007). The rift-to-drift transition in the North Atlantic: A stuttering start of the MORB machine? *Geology*, 35(12):1087–1090.

Jagoutz, O., Müntener, O., Schmidt, M. W., and Burg, J.-P. (2011). The roles of flux- and decompression melting and their respective fractionation lines for continental crust formation: Evidence from the Kohistan arc. *Earth and Planetary Science Letters*, 303:25–36.

Jammes, S., Manatschal, G., Lavier, L., and Masini, E. (2009). Tectonosedimentary evolution related to extreme crustal thinning ahead of a propagating ocean: Example of the western Pyrenees. *Tectonics*, 28(4):TC4012.

Jarrard, R. D. (1986). Relations among subduction parameters. *Reviews of Geophysics*, 24(2):217–284.

Kaus, B. J., Connolly, J. A., Podladchikov, Y. Y., and Schmalholz, S. M. (2005). Effect of mineral phase transitions on sedimentary basin subsidence and uplift. *Earth and Planetary Science Letters*, 233(1-2):213–228.

Klingelhöfer, F., Edwards, R. A., Hobbs, R. W., and England, R. W. (2005). Crustal structure of the NE Rockall Trough from wide-angle seismic data modeling. *Journal of Geophysical Research*, 110(B11):B11105.

Krabbendam, M. and Barr, T. D. (2000). Proterozoic orogens and the break-up of Gondwana: why did some orogens not rift? *Journal of African Earth Sciences*, 31(1):35–49.

Kröner, U. and Romer, R. (2013). Two plates – Many subduction zones: The Variscan orogeny reconsidered. *Gondwana Research*, 24(1):298–329.

Kvarven, T. (2013). *On the evolution of the North Atlantic - from continental collapse to oceanic accretion*. PhD thesis, University of Bergen, Bergen, Norway.

Lacassin, R., Tapponnier, P., and Bourjo, L. (1990). Culminations anticlinales d'échelle crustale et imbrication de la lithosphère dans les Alpes, apports du profil ECORS-CROP. *Comptes rendus de l'Académie des sciences*, 310:807–814.

Latin, D. and White, N. (1990). Generating melt during lithospheric extension: Pure shear vs. simple shear. *Geology*, 18:327–331.

Lemoine, M., Tricart, P., and Boillot, G. (1987). Ultramafic and gabbroic ocean floor of the Ligurian Tethys (Alps, Corsica, Apennines): In search of a genetic imodel. *Geology*, 15(7):622–625.

Leroy, S., Lucazeau, F., D'Acremont, E., Watremez, L., Autin, J., Rouzo, S., Bellahsen, N., Tiberi, C., Ebinger, C., Beslier, M. O., Perrot, J., Razin, P., Rolandone, F., Sloan, H., Stuart, G., Lazki, A. A., Al-Toubi, K., Bache, F., Bonneville, A., Goutorbe, B., Huchon, P., Unternehr, P., and Khanbari, K. (2010). Contrasted styles of rifting in the eastern Gulf of Aden: A combined wide-angle, multichannel seismic, and heat flow survey. *Geochemistry, Geophysics, Geosystems*, 11(7):1–14.

Lester, R., Van Avendonk, H. J. a., Mcintosh, K., Lavier, L., Liu, C.-S., Wang, T. K., and Wu, F. (2014). Rifting and magmatism in the northeastern South China Sea from wide-angle tomography and seismic reflection imaging. *Journal of Geophysical Research*, 119:2305–2323.

Mac Niocaill, C., Van der Pluijm, B. A., and Van der Voo, R. (1997). Ordovician paleogeography and the evolution of the Iapetus ocean. *Geology*, 25(2):159–162.

Manatschal, G., Lavier, L., and Chenin, P. (2015). The role of inheritance in structuring hyperextended rift systems: Some considerations based on observations and numerical modeling. *Gondwana Research*, 27(1):140–164.

Manatschal, G. and Müntener, O. (2009). A type sequence across an ancient magma-poor ocean–continent transition: the example of the western Alpine Tethys ophiolites. *Tectonophysics*, 473:4–19.

Martinez, F. and Taylor, B. (2002). Mantle wedge control on back-arc crustal accretion. *Nature*, 416(6879):417–420.

Mattauer, M. (1968). Les traits structuraux essentiels de la chaîne pyrénéenne. *Revue de Géologie Dynamique et de Géographie physique*, 10:3–11.

Matte, P. (2001). The Variscan collage and orogeny (480- 290 Ma) and the tectonic definition of the Armorica microplate: a review. *Terra Nova*, 13:122–128.

McCarthy, A. and Müntener, O. (2015). Ancient depletion and mantle heterogeneity: Revisiting the Permian-Jurassic paradox of Alpine peridotites. *Geology*, 43(3):255–258.

McClay, K. R., Norton, M. G., Coney, P., and Davis, G. H. (1986). Collapse of the Caledonian orogen and the Old Red Sandstone. *Nature*, 323:147–149.

McDermott, K., Bellingham, P., Pindell, J., Graham, R., and Horn, B. (2014). Some insights into rifted margin development and the structure of the continent-ocean transition using a global deep seismic reflection database. In *4th Atlantic Conjugate Margins Conference*, pages 62–65, St John's.

McKerrow, W. S., Mac Niocaill, C., Ahlberg, P. E., Clayton, G., Cleal, C. J., and Eagar, R. M. C. (2000a). The Late Palaeozoic relations between Gondwana and Laurussia. *Geological Society, London, Special Publications*, 179(1):9–20.

McKerrow, W. S., Mac Niocaill, C., and Dewey, J. F. (2000b). The Caledonian Orogeny redefined. *Journal of the Geological Society*, 157(6):1149–1154.

Meissner, R. (1999). Terrane accumulation and collapse in central Europe: seismic and rheological constraints. *Tectonophysics*, 305(1-3):93–107.

Mengel, K. and Kern, H. (1992). Evolution of the petrological and seismic Moho – implications for the continental crust-mantle boundary. *Terra Nova*, 4(1):109–116.

Mével, C. (2003). Serpentinization of abyssal peridotites at mid-ocean ridges. *Comptes Rendus Geoscience*, 335(10-11):825–852.

Miller, D. J. and Christensen, N. I. (1997). Seismic velocities of lower crustal and upper mantle rocks from the slow-spreading Mid-Atlantic Ridge, south of the Kane Transform Zone (MARK). *Proceedings of the Ocean Drilling Program. Scientific results*, 153:437–454.

Minshull, T. a., Muller, M. R., Robinson, C. J., White, R. S., and Bickle, M. J. (1998). Is the oceanic Moho a serpentinization front? *Geological Society, London, Special Publications*, 148(1):71–80.

Miyashiro, A. (1961). Evolution of Metamorphic Belts. *Journal of Petrology*, 2(3):277–311.

Miyashiro, A. (1967). Orogeny, regional metamorphism, and magmatism in the Japanese Islands. *Medd. fra Dansk Geol. Forening*, 17:390–446.

Mohn, G., Manatschal, G., Beltrando, M., and Haupert, I. (2014). The role of rift-inherited hyper-extension in Alpine-type orogens. *Terra Nova*, 26(5):347–353.

Mohn, G., Manatschal, G., Masini, E., and Müntener, O. (2011). Rift-related inheritance in orogens: a case study from the Austroalpine nappes in Central Alps (SE-Switzerland and N-Italy). *International Journal of Earth Sciences*, 100(5):937–961.

Mohn, G., Manatschal, G., Müntener, O., Beltrando, M., and Masini, E. (2010). Unravelling the interaction between tectonic and sedimentary processes during lithospheric thinning in the Alpine Tethys margins. *International Journal of Earth Sciences*, 99:75–101.

Muñoz, J. A. (1992). Evolution of a continental collision belt: ECORS-Pyrenees crustal. In *Thrust tectonics*, pages 235–246. Springer.

771 Müntener, O., Manatschal, G., Desmurs, L., and Pettke, T. (2010). Plagioclase peridotites
772 in ocean-continent transitions: Refertilized mantle domains generated by melt stagnation
773 in the shallow mantle lithosphere. *Journal of Petrology*, 51(1-2):255–294.

774 Müntener, O., Pettke, T., Desmurs, L., Meier, M., and Schaltegger, U. (2004). Refertil-
775 ization of mantle peridotite in embryonic ocean basins: trace element and Nd isotopic
776 evidence and implications for crust-mantle relationships. *Earth and Planetary Science*
777 *Letters*, 221:293–308.

778 Müntener, O. and Piccardo, G. B. (2003). Melt migration in ophiolitic peridotites: the
779 message from Alpine-Apennine peridotites and implications for embryonic ocean basins.
780 *Geological Society, London, Special Publications*, 218(1):69–89.

781 Nance, R. D. and Linnemann, U. (2008). The Rheic Ocean: Origin, evolution, and signif-
782 icance. *GSA Today*, 18(12):4.

783 Nicolas, A., Hirn, A., Nicolich, R., and Polino, R. (1990). Lithospheric wedging in the
784 western Alps inferred from the ECORS-CROP traverse. *Geology*, 18(7):587–590.

785 Nirrengarten, M., Gernigon, L., and Manatschal, G. (2014). Nature, structure and age
786 of Lower Crustal Bodies in the Møre volcanic rifted margin: facts and uncertainties.
787 *Tectonophysics*, 636:143–157.

788 Osmundsen, P. T. and Ebbing, J. (2008). Styles of extension offshore mid-Norway and
789 implications for mechanisms of crustal thinning at passive margins. *Tectonics*, 27(6).

790 Peacock, S. M. (1991). Numerical simulation of subduction zone pressure-temperature-time
791 paths: Constraints on fluid production and arc magmatism. *Philosophical Transactions*
792 *of the Royal Society of London A: Mathematical, Physical and Engineering Sciences*,
793 335(1638):341–353.

794 Peacock, S. M., Rushmer, T., and Thompson, A. B. (1994). Partial melting of subducting
795 oceanic crust. *Earth and Planetary Science Letters*, 121(1-2):227–244.

796 Pérez-Gussinyé, M., Ranero, C. R., and Reston, T. J. (2003). Mechanisms of extension at
797 nonvolcanic margins: Evidence from the Galicia interior basin, west of Iberia. *Journal*
798 *of Geophysical Research*, 108(B5).

799 Péron-Pinvidic, G., Manatschal, G., and Osmundsen, P. T. (2013). Structural comparison
800 of archetypal Atlantic rifted margins: A review of observations and concepts. *Marine*
801 *and Petroleum Geology*, 43:21–47.

Petri, B. (2014). *Formation et exhumation des granulites permiennes*. PhD thesis, Université de Strasbourg.

Picazo, S., Cannat, M., Delacour, A., Escartín, J., Rouméjon, S., and Silantyev, S. (2012). Deformation associated with the denudation of mantle-derived rocks at the Mid-Atlantic Ridge 13°-15°N: The role of magmatic injections and hydrothermal alteration. *Geochemistry, Geophysics, Geosystems*, 13(9):n/a–n/a.

Picazo, S., Manatschal, G., Cannat, M., and Andréani, M. (2013). Deformation associated to exhumation of serpentinized mantle rocks in a fossil Ocean Continent Transition: The Totalp unit in SE Switzerland. *Lithos*, 175-176:255–271.

Picazo, S., Müntener, O., Manatschal, G., Bauville, A., Karner, G. D., and Johnson, C. (2016). Mapping the nature of mantle domains in Western and Central Europe based on clinopyroxene and spinel chemistry: evidence for mantle modification during an extensional cycle. *Lithos*.

Pinto, V. H. (2014). *Linking tectonic evolution with fluid history in hyperextended rifted margins: Examples from the fossil Alpine and Pyrenean rift systems and the present-day Iberia rifted margin*. PhD thesis, Université de Strasbourg.

Pognante, U., Perotto, A., Salino, C., and Toscani, L. (1986). The ophiolitic peridotites of the Western Alps: Record of the evolution of a small oceanic-type basin in the Mesozoic Tethys. *TMPM Tschermaks Mineralogische und Petrographische Mitteilungen*, 35:47–65.

Radhakrishna, M., Twinkle, D., Nayak, S., Bastia, R., and Rao, G. S. (2012). Crustal structure and rift architecture across the Krishna-Godavari basin in the central Eastern Continental Margin of India based on analysis of gravity and seismic data. *Marine and Petroleum Geology*, 37(1):129–146.

Reston, T., Gaw, V., Pennell, J., Klaeschen, D., Stubenrauch, A., and Walker, I. (2004). Extreme crustal thinning in the south Porcupine Basin and the nature of the Porcupine Median High: implications for the formation of non-volcanic rifted margins. *Journal of the Geological Society*, 161:783–798.

Rey, P. (1993). Seismic and tectono-metamorphic characters of the lower continental crust in Phanerozoic areas: a consequence of post-thickening extension. *Tectonics*, 12(2):580–590.

832 Roberts, D. (2003). The Scandinavian Caledonides: event chronology, palaeogeographic
833 settings and likely modern analogues. *Tectonophysics*, 365:283–299.

834 Roca, E., Muñoz, J. A., Ferrer, O., and Ellouz, N. (2011). The role of the Bay of Biscay
835 Mesozoic extensional structure in the configuration of the Pyrenean orogen: Constraints
836 from the MARCONI deep seismic reflection survey. *Tectonics*, 30:TC2001.

837 Rosenbaum, G. and Lister, G. S. (2005). The Western Alps from the Jurassic to Oligocene:
838 Spatio-temporal constraints and evolutionary reconstructions. *Earth-Science Reviews*,
839 69(3-4):281–306.

840 Rosenbaum, G., Lister, G. S., and Duboz, C. (2002). Relative motions of Africa, Iberia
841 and Europe during Alpine orogeny. *Tectonophysics*, 359(1-2):117–129.

842 Roure, F., Choukroune, P., and Polino, R. (1996). Deep seismic reflection data and new
843 insights on the bulk geometry of mountain ranges. *Comptes rendus de l'Académie des*
844 *sciences*, 322:345–359.

845 Rüpke, L. H., Morgan, J. P., Hort, M., and Connolly, J. A. D. (2004). Serpentine and the
846 subduction zone water cycle. *Earth and Planetary Science Letters*, 223(1-2):17–34.

847 Schaltegger, U. (1997). Magma pulses in the Central Variscan Belt: episodic melt genera-
848 tion and emplacement during lithospheric thinning. *Terra Nova*, 9(5/6):242–245.

849 Schmid, S. M., Fgenschuh, B., Kissling, E., Schuster, R., and Fügenschuh, B. (2004).
850 Tectonic map and overall architecture of the Alpine orogen. *Eclogae Geologicae Helvetiae*,
851 97:93–117.

852 Schmid, S. M. and Kissling, E. (2000). The arc of the western Alps in the light of geophys-
853 ical data on deep crustal structure. *Tectonics*, 19:62–85.

854 Sclater, J. G., Jaupart, C., and Galson, D. (1980). The heat flow through oceanic and
855 continental crust and the heat loss of the Earth. *Reviews of Geophysics*, 18(1):269.

856 Sisson, T. W. and Bronto, S. (1998). Evidence for pressure-release melting beneath mag-
857 matic arcs from basalt at Galunggung, Indonesia. *Nature*, 391(1996):883–886.

858 Skelton, A., Whitmarsh, R., Arghe, F., Crill, P., and Koyi, H. (2005). Constraining the rate
859 and extent of mantle serpentinization from seismic and petrological data: implications
860 for chemosynthesis and tectonic processes. *Geofluids*, 5(3):153–164.

Skogseid, J. (2010). The Orphan Basin - a key to understanding the kinematic linkage between North and NE Atlantic Mesozoic rifting. *II Central and North Atlantic Conjugate Margins Conference*, II:13–23.

Stern, C. R. (2011). Subduction erosion: Rates, mechanisms, and its role in arc magmatism and the evolution of the continental crust and mantle. *Gondwana Research*, 20:284–308.

Stern, R. J. (2002). Subduction zones. *Reviews of Geophysics*, 40(4):3.1–3.13.

Stern, R. J. (2004). Subduction initiation: spontaneous and induced. *Earth and Planetary Science Letters*, 226:275–292.

Stevenson, D. J. and Turner, J. S. (1977). Angle of subduction. *Nature*, 270(5635):334–336.

Stica, J. M., Zalán, P. V., and Ferrari, A. L. (2014). The evolution of rifting on the volcanic margin of the Pelotas Basin and the contextualization of the Paraná-Etendeka LIP in the separation of Gondwana in the South Atlantic. *Marine and Petroleum Geology*, 50:1–21.

Sutra, E., Manatschal, G., Mohn, G., and Unternehr, P. (2013). Quantification and restoration of extensional deformation along the Western Iberia and Newfoundland rifted margins. *Geochemistry, Geophysics, Geosystems*, 14(8):2575–2597.

Thouvenot, F., Senechal, G., Truffert, C., and Guellec, S. (1996). Comparison between two techniques of line-drawing migration (ray-tracing and common tangent method). *Mémoires Société Géologique de France*, 170:53–59.

Torsvik, T. H. (1998). Palaeozoic palaeogeography: A North Atlantic viewpoint. *GFF*, 120:109–118.

Tovish, A., Schubert, G., and Luyendyk, B. P. (1978). Mantle flow pressure and the angle of subduction: Non-Newtonian corner flows. *Journal of Geophysical Research*, 83(B12):5892.

Tugend, J., Manatschal, G., and Kusznir, N. (2015). Spatial and temporal evolution of hyperextended rift systems: implication for the nature, kinematics and timing of the Iberian-European plate boundary. *Geology*, 43(1):15–18.

Unternehr, P., Péron-Pinvidic, G., Manatschal, G., and Sutra, E. (2010). Hyper-extended crust in the South Atlantic: in search of a model. *Petroleum Geoscience*, 16(3):207–215.

Uyeda, S. (1981). Subduction zones and back arc basins - A review. *Geologische Rundschau*, 70(2):552–569.

van Staal, C. R., Barr, S. M., and Murphy, J. B. (2012). Provenance and tectonic evolution of Ganderia: Constraints on the evolution of the Iapetus and Rheic oceans. *Geology*, 40(11):987–990.

Vanderhaeghe, O. and Teyssier, C. (2001). Crustal-scale rheological transitions during late-orogenic collapse. *Tectonophysics*, 335:211–228.

Vlaar, N. J. and Cloetingh, S. A. P. L. (1984). Orogeny and ophiolites: plate tectonics revisited with reference to the Alps. In Zwart, H. J., Hartman, P., and Tobi, A. C., editors, *Ophiolites and ultramafic rocks – a tribute to Emile den Tex – Geol. Mijnbouw 63*, pages 159–164.

Welford, J. K., Shannon, P. M., O'Reilly, B. M., and Hall, J. (2010). Lithospheric density variations and Moho structure of the Irish Atlantic continental margin from constrained 3-D gravity inversion. *Geophysical Journal International*, 183:79–95.

Whitmarsh, R. B., Manatschal, G., and Minshull, T. a. (2001). Evolution of magma-poor continental margins from rifting to seafloor spreading. *Nature*, 413(6852):150–154.

Willett, S., Beaumont, C., and Fullsack, P. (1993). Mechanical model for the tectonics of doubly vergent compressional orogens. *Geology*, 21(4):371–374.

Withjack, M. O., Schlische, R. W., and Olsen, P. E. (1998). Diachronous rifting, drifting, and inversion on the passive margin of central Eastern North America: An analog for other passive margins. *AAPG Bulletin*, 82(5):817–835.

Woodhead, J., Eggins, S., and Gamble, J. (1993). High field strength and transition element systematics in island arc and back-arc basin basalts: Evidence for multi-phase melt extraction and a depleted mantle wedge. *Earth and Planetary Science Letters*, 114(4):491–504.

Workman, R. K. and Hart, S. R. (2005). Major and trace element composition of the depleted MORB mantle (DMM). *Earth and Planetary Science Letters*, 231(1-2):53–72.

Zalán, P. V., Severino, M. D. C. G., Rigoti, C. A., Magnavita, L. P., Bach de Oliveira, J. A., and Viana, A. R. (2012). 3D crustal architecture of a magma-poor passive margin, Santos, Campos and Espírito Santo Basins – Comparisons with a volcanic passive margin, Pelotas Basin – Offshore Brazil. *Marine and Petroleum Geology*.

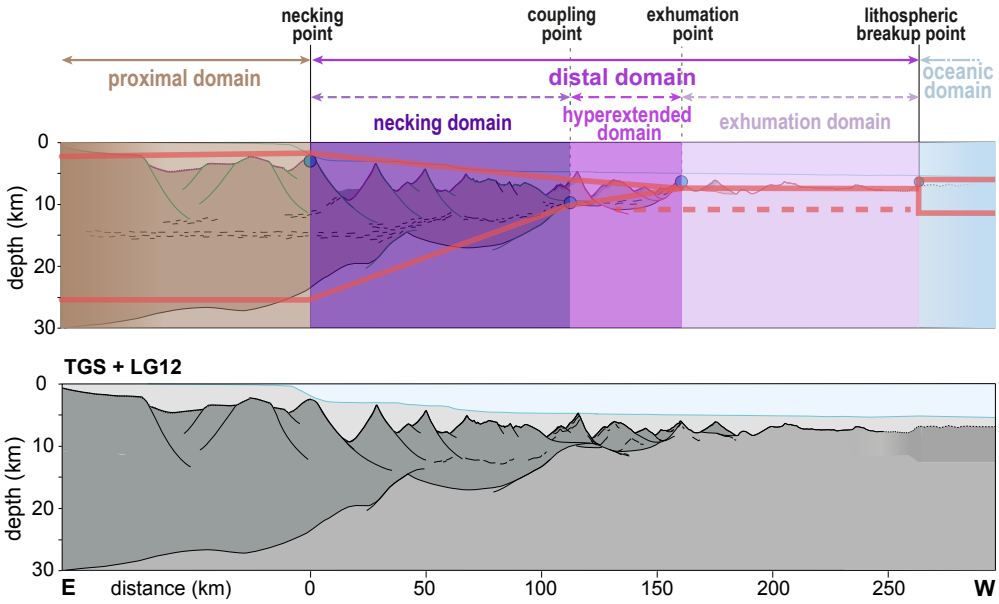

Figure 1: Definition of rift (sub-)domains based on Sutra et al. (2013) and Chenin et al. (2015) and their first-order morphology (red lines). The dashed line represents the 'seismic Moho' (i.e. a sharp increase in P velocity from < 7 km.s^{-1} to > 7.8 km.s^{-1}; see Mengel and Kern (1992)), where it differs from the petrologic Moho (i.e. the crust–mantle boundary).

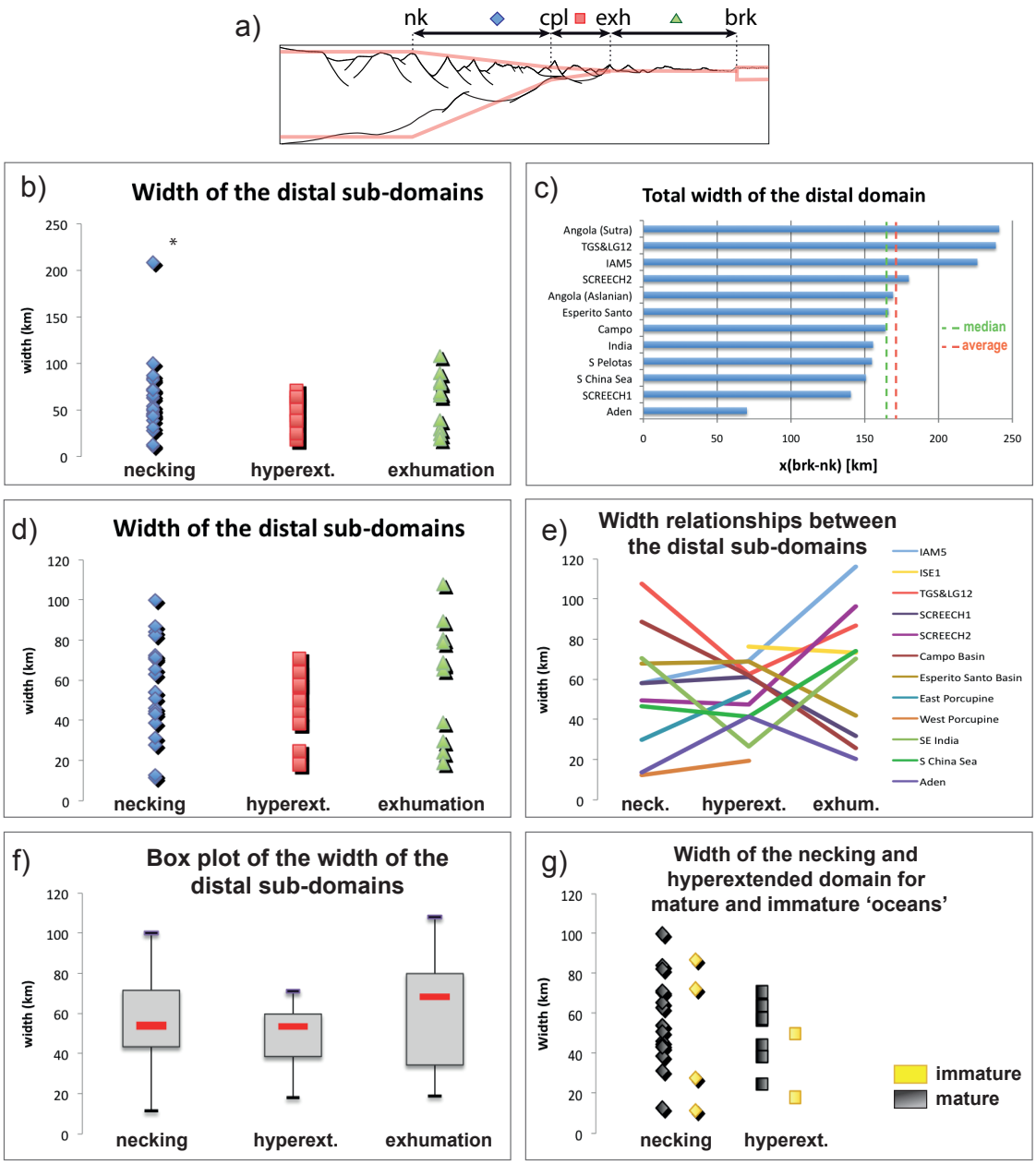

Figure 2: (a) Definition of the necking (blue diamond), hyperextended (red square) and exhumation (green triangle) domains; nk: necking point; cpl: coupling point; exh: exhumation point; brk: lithospheric breakup point. (b) Width of the necking, hyperextended and exhumation domains for all selected margins; (c) Total width of the distal domain for several rifted margins; (d) Width of the necking, hyperextended and exhumation domains without the anomalously wide necking domain of the ISE1 section (see text for discussion); (e) Width relationships between the necking, hyperextended and exhumation domains; (f) Box plot of the width of the necking, hyperextended and exhumation domains; (g) Width of the necking and hyperextended domains for immature and mature oceans.

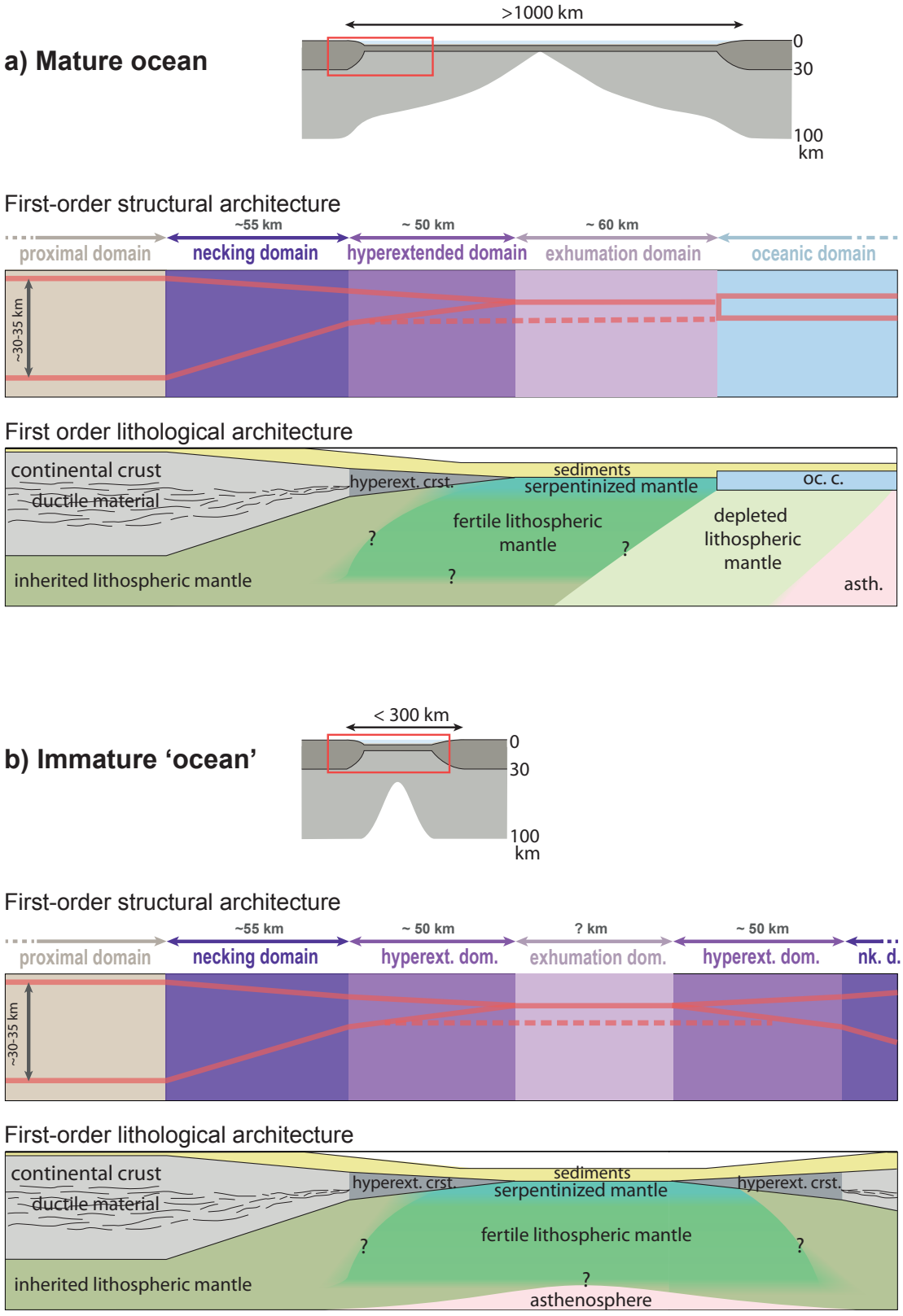

Figure 3: First-order architecture of magma-poor hyperextended rifted margins from (a) wide, mature oceans; and (b) narrow, immature oceans. Abbreviations: nk. d.: necking domain; hyperext. crst.: hyperextended continental crust; oc. c.: oceanic crust; asth.: asthenospheric mantle. See text for discussion.

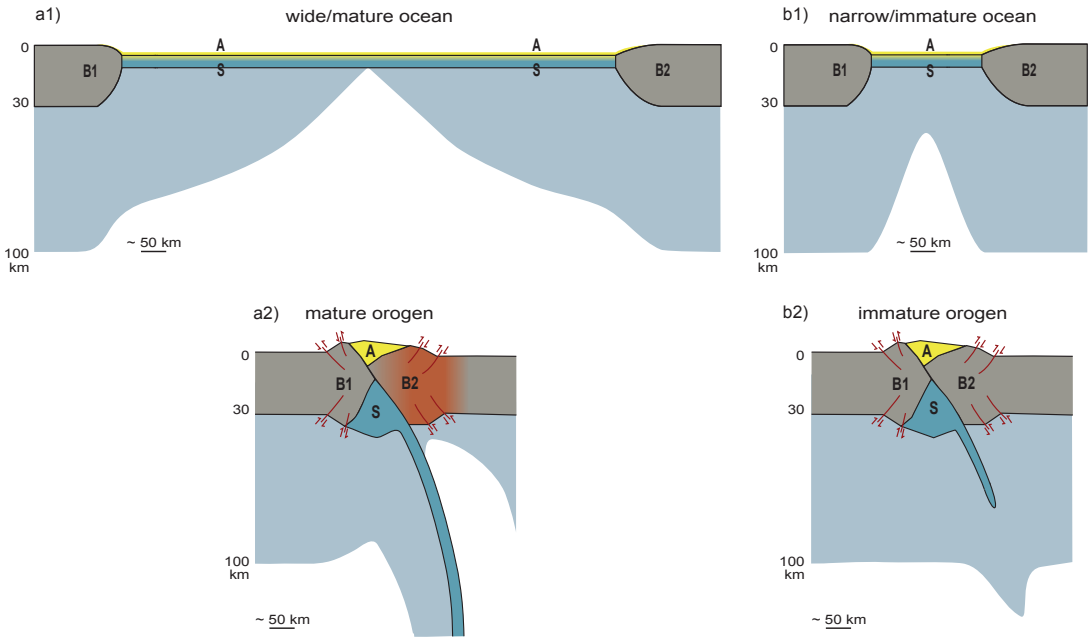

Figure 4: First-order architecture of a (a1) wide mature ocean; and (b1) narrow immature ocean. First-order architecture of (a2) a mature orogen following the subduction of a wide ocean; and (b2) an immature orogen produced by the closure of a narrow ocean; In both cases, continental collision involves two buttresses B (external parts of the orogen), an accretionary prism A (internal part of the orogen) and a subducted part S.

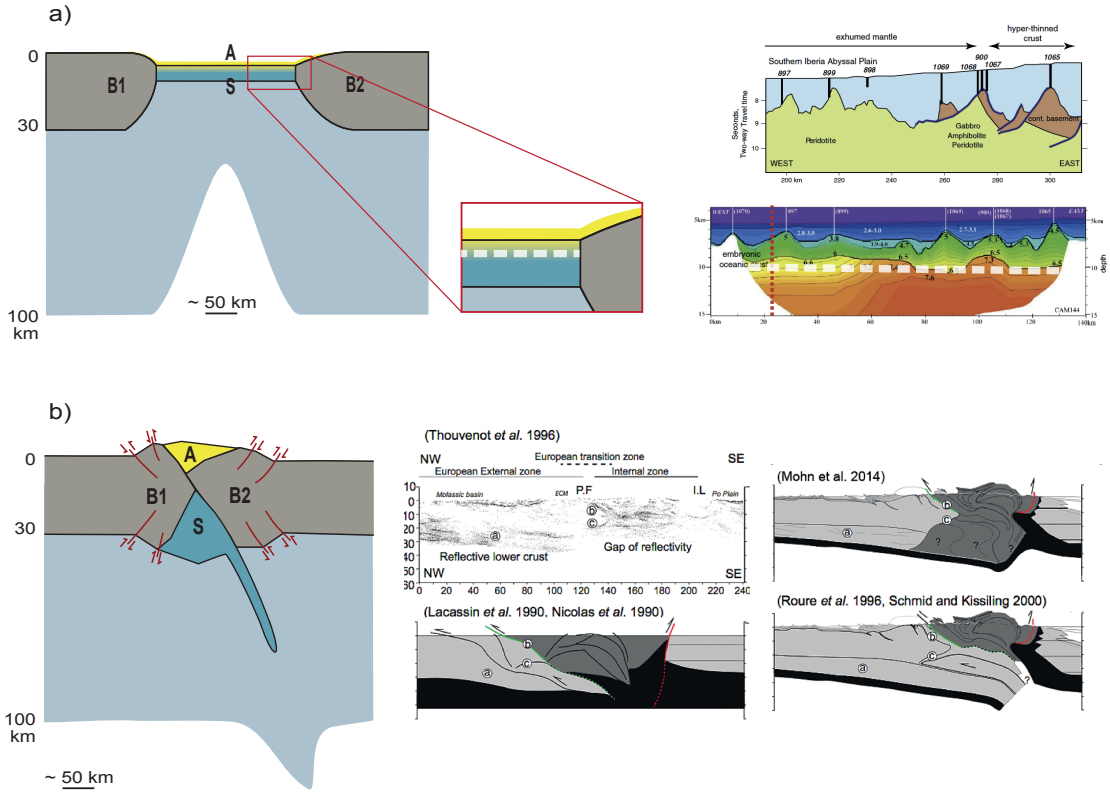

Figure 5: (a) The decoupling level between the subducted and accreted material during subduction corresponds possibly to the hydration front based on the geological interpretation of the reflection Lusigal 12 seismic section and the Velocity model of the adjacent CAM 144 seismic section by Beltrando et al. (2014). (b) Uncertainty about the nature of the deep structure of collisional orogens highlighted by the various interpretations of the ECORS-CROP seismic profile through the Alpine orogen (from Mohn et al., 2014).

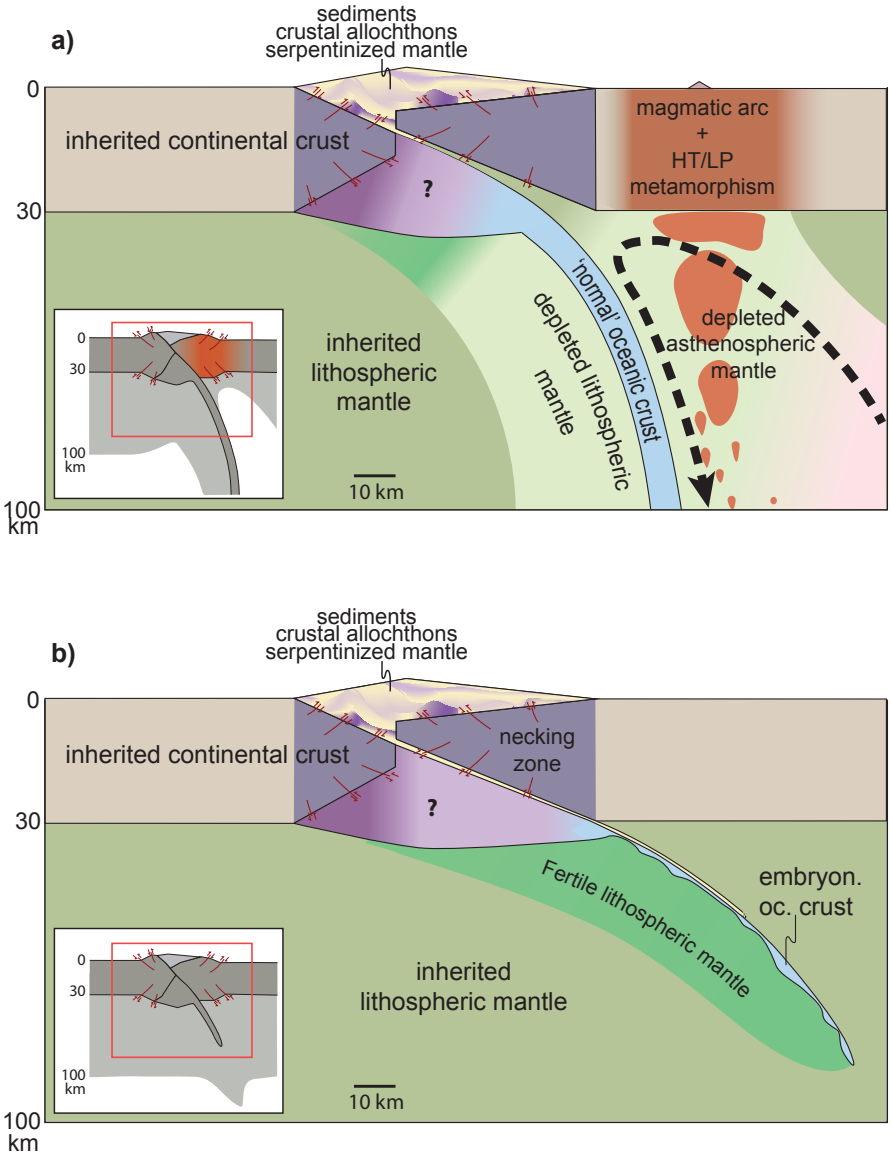

Figure 6: Architecture of orogens following the closure of a (a) wide and mature ocean; and (b) narrow and immature ocean. The inserts highlight the scale of the zones represented. Abbreviations: embryon. oc.: embryonic oceanic crust; HT/LP: high temperature/low pressure.

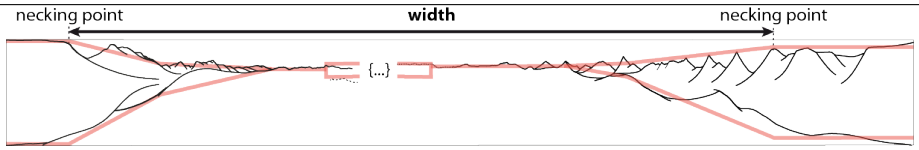

	Width	Basin floor	References
Atlantic Ocean	$\sim$ 3,000 - 5,000 km	oceanic crust	
Porcupine Basin	$<$ 200 km	thinned cont. crust (& exhumed mantle?)	Reston et al. (2004)
Rockall Trough	$\sim$ 250 km	thinned cont. crust	Klingelhöfer et al. (2005)
Hatton Basin	$\sim$ 200 km	thinned cont. crust	Edwards (2002)
Orphan Basin	$\sim$ 400 km	thinned cont. crust	Chian et al. (2001)
Northern Red Sea	250–350 km	no or embryonic oceanic crust	Bosworth et al. (2005)
Southern Red Sea	350–450 km	no or embryonic oceanic crust	Bosworth et al. (2005)
Gulf of Aden	$<$ 200 km	(embryonic?) oc. crust	Bosworth et al. (2005)
Indian Ocean	up to $\sim$ 20,000 km	oceanic crust	
Pacific Oean	up to $\sim$10,000 km	oceanic crust	

Table 1: Width and nature of basement floor of several present-day extensional systems. The *width* refers to the distance between the two conjugate necking points (nk).

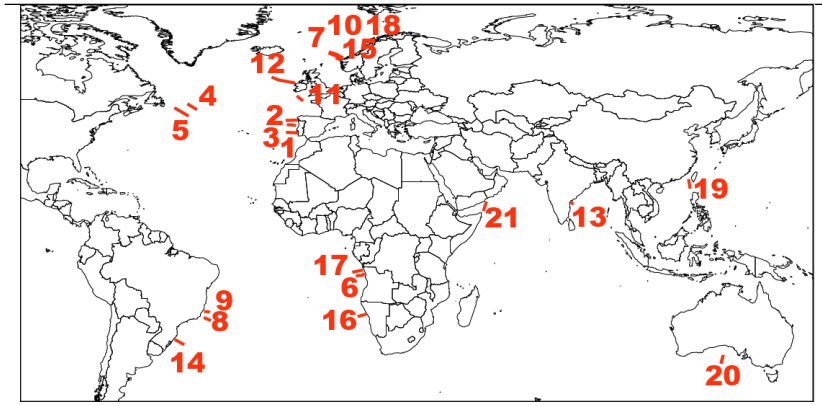

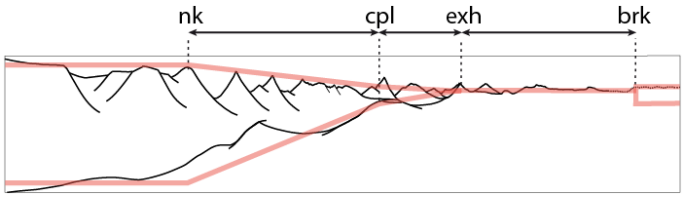

	Seismic section	x(cpl-nk) (km)	x(exh-cpl) (km)	x(brk-exh) (km)	x(brk-nk) (km)	Moho and basement linedrawing
1	IAM5 (Afilhado et al., 2008)	54	64	108	226	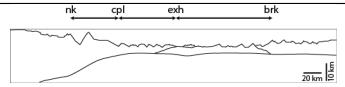
2	ISE1 (Sutra et al., 2013)	208*	71	68	347	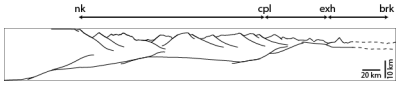
3	TGS+LG12 (Sutra et al., 2013)	100	58	81	239	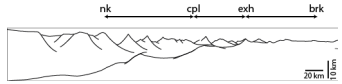
4	SCREECH1 (Sutra et al., 2013)	54	57	30	141	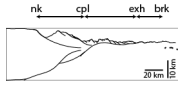
5	SCREECH2 (Sutra et al., 2013)	46	44	90	180	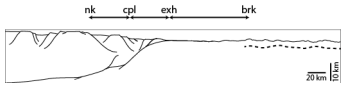
6	Angola (Unternehr et al., 2010)	71			241	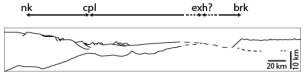

	Seismic section	x(cpl-nk)	x(exh-cpl)	x(brk-exh)	x(brk-nk)	Moho and basement linedrawing
7	Norway (TrII Nirrengarten et al., 2014)	84				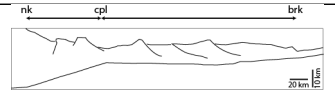
8	Campos Basin (Zalán et al., 2012)	82	58	24	164	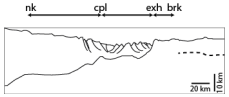
9	Esperito Santo Basin (Zalán et al., 2012)	63	64	39	166	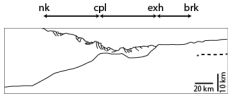
10	Norway (Osmundsen and Ebbing, 2008)	45				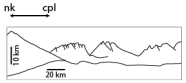
11	E-Porcupine (McDermott et al., 2014)	28	50			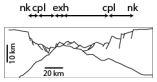
11	W-Porcupine (McDermott et al., 2014)	11	18			
12	E-Rockall (Welford et al., 2010)	72				
12	W-Rockall (Welford et al., 2010)	87				
13	India (Radhakrishna et al., 2012)	65	25	65	156	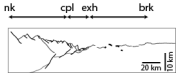
14	S-Pelotas (Stica et al., 2014)	71			155	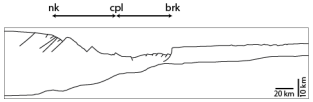
15	Norway (Kvarven, 2013)	43				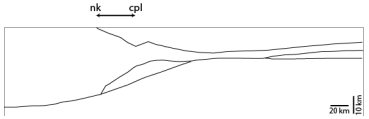
16	Namibia (Gladczenko et al., 1998)	51				

	Seismic section	x(cpl-nk)	x(exh-cpl)	x(brk-exh)	x(brk-nk)	Moho and basement linedrawing
17	Angola (Aslanian et al., 2009)	39			169	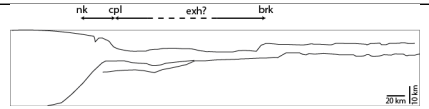
18	Norway (Osmundsen and Ebbing, 2008)	31				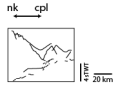
19	China Sea (Lester et al., 2014)	43	39	69	151	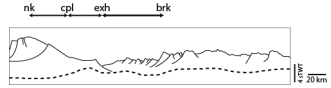
20	South Australia (Direen et al., 2008)			79		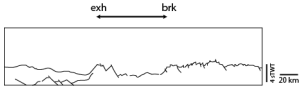
21	Aden (Leroy et al., 2010)	13	39	19	70	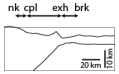

Table 2: Width of the marginal domains for several hyperextened to oceanic rift systems. nk: necking point; cpl: coupling point; exh: exhumation point; brk: breakup point (see Figure 1).

temp. (°C)	700			800			900		
mantle type	harz.	fertile lherz.		harz.	fertile lherz.		harz.	fertile lherz.	
P (GPa)		**(plg)**			**(plg)**			**(plg)**	
0.5	3.260	3.209		3.248	3.197	**(spl)**	3.235	3.185	**(spl)**
1	3.275	3.224	**(spl)**	3.263	3.213	3.276	3.250	3.201	3.264
1.5	3.295		3.303	3.283		3.291	3.271		3.279
2	3.309		3.317	3.297		3.306	3.300	**(grt)**	3.310
2.5	3.323	**(grt)**	3.331	3.311	**(grt)**	3.320	3.299	3.332	3.308
3	3.336	3.368		3.325	3.357		3.313	3.346	

temp. (°C)	1000			1100			1200		
mantle type	harz.	fertile lherz.		harz.	fertile lherz.		harz.	fertile lherz.	
P (GPa)		**(plg)**			**(plg)**			**(plg)**	
0.5	3.222	3.173	**(spl)**	3.209	3.161	**(spl)**	3.195	3.148	**(spl)**
1	3.237	3.189	3.251	3.225	3.177	3.239	3.212	3.165	3.226
1.5	3.258		3.267	3.246		3.254	3.233		3.242
2	3.273	**(grt)**	3.282	3.261	**(grt)**	3.270	3.249	**(grt)**	3.258
2.5	3.288	3.320	3.297	3.276	3.309	3.285	3.264	3.297	3.273
3	3.300	3.334		3.288	3.323		3.277	3.312	

temp. (°C)	1300	
mantle type	harz.	lherz.
P (GPa)		
0.5		
1		
1.5		**(spl)**
2	3.236	3.246
2.5	3.250	3.262
		(grt)
3	3.265	3.300

Table 3: Density in the mantle as a function of temperature. pressure and composition calculated with the algorithms of Hacker et al. (2003). Depleted harzburgite (harz.): 80% olivine, 20% opx, both with a Mg# of 90-91; Fertile plagioclase peridotite (plg fertile lherz.): 9% plagioclase (An80), 60% olivine (Fo90), 24% opx (Mg# 90), 7% cpx (Mg# 90); Fertile spinel peridotite (spl fertile lherz.): 2% spinel (spinel, hercynite, magnetite), 58% olivine (Fo90), 26% opx (Mg# 90), 14% cpx (Mg# 90); Fertile garnet peridotite (grt fertile lherz.): 9% garnet (pyrope 66%, almandin 24%, grossular 10%), 60% olivine (Fo89), 24% opx (Mg#89), 7% cpx (Mg# 90).

	Narrow 'ocean'	Wide ocean
Spatial extent	$\lesssim$ 350–400 km	$>$ 1,000 km
Oceanic crust	unsteady seafloor spreading $\Rightarrow$ rough, heterogeneous in thickness and composition; no mantle depletion	steady-state seafloor spreading $\Rightarrow$ smooth, homogeneous in thickness and composition; depleted underlying mantle
Magmatic activity	none or very little $\Rightarrow$ no mantle depletion	moderate to large $\Rightarrow$ mantle depletion
Subduction geometry	shallow angle	shallow or deep angle
Subduction sustainability	transitory	self-sustained
Mantle wedge convection	minor	vigorous
Magmatic arc	none	yes; new over-thickened crust creation and associated HT metamorphism and underlying mantle depletion
backarc basin	none	possible; may be associated with seafloor spreading and underlying mantle depletion
Orogen type	collisional	accretionary followed by collisional
Mantle wedge composition	hydrated and fertilized with sediments	Depleted in fusible elements
Post-orogenic collapse	possibly magmatic	purely extensional

Table 4: Summary of the characteristics of narrow versus wide extensional systems, subduction processes and orogens (see text for discussion).